Synthetic images of the vicinity of black holes with efficient ray-tracing techniques

Talk by: Ezequiel F. Boero
Collaborator: Osvaldo M. Moreschi

Universidad Nacional de Córdoba,
Inst. de Astronomía Teórica y Experimental, (IATE), CONICET,
Inst. de Física Enrique Gaviola (IFEG), CONICET,
(5000) Córdoba, Argentina

Verão Quântico
Espirito Santo, Brazil - April 14th, 2023

Motivations I

- We've been interested in various aspects of gravitational lensing phenomena:
  - Geometries allowing a more general description of DM without a priori physical assumptions within the framework of GR [GM12, BM18]
  - Effects of plasma environments on strong lensing [CGBM22].
  - Lensing in the strong field regime (typically BHs) and lenses with angular momentum [BM20, BM21].
  - Weak lensing signatures in voids and gravitational lensing in the CMB.
- Recent achievements from the Event Horizon Telescope in the vicinity of SMBHs.
- Upcoming data of lensed systems in the low radio frequency regime such as those expected to be observed in LOFAR+nenuFAR observatory.

Introduction I

- This talk: Introduce a new very simple and compact expression that allows for an efficient calculation of gravitational lens optical scalars in Kerr spacetime that improves the standard ray-tracing often used.

  It is exact and valid for any null geodesic.

  Its derivation is based on well-known results on geodesic motion that exploit obvious and hidden symmetries of Kerr spacetime and contrast with the rather long and cumbersome expressions previously reported in the literature.

- We will apply this formula to study images produced by an accretion disc in the vicinity of of a SMBH.

  We will use a simple emission profile for the orbiting plasma (using very little input from GRMHD) and we will investigate to what extent one can reproduce the images released by the EHT Collaboration.

Gravitational lensing and black holes

Angular variables

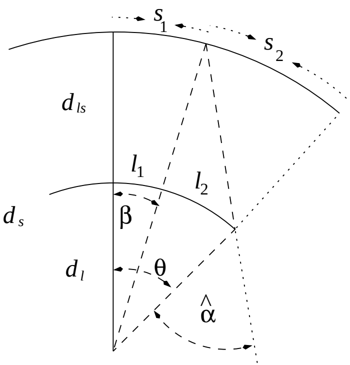

Lens equation and optical scalars

$$\beta^a = \theta^a - \frac{d_{ls}}{d_s}\alpha^a,$$

$$\delta\beta^a = \mathcal{A}^a{}_b\,\delta\theta^b,$$

$$\mathcal{A}^a{}_b = \begin{pmatrix} 1-\kappa-\gamma_1 & -\gamma_2-\omega \\ -\gamma_2+\omega & 1-\kappa+\gamma_1 \end{pmatrix}.$$

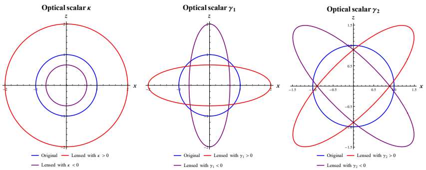

- One compares with respect to the flat spacetime and we retain the basic notions:
  - θ is the observed angle (i.e. non-trivial curvature)
  - β is the angle that one would observe without lens (i.e. no curvature).
  - The distance to the source in terms of the affine distance λ.

Gravitational lensing II

Angular variables

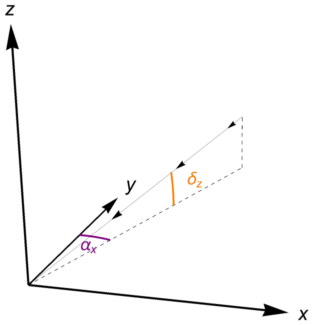

(α_x, δ_z) is a pair of observing angle for the incoming photons w.r.t. an orthogonal tetrad $(\hat{T}^a, \hat{X}^a, \hat{Y}^a, \hat{Z}^a)$ at the observer position

Geodesic deviation equation

Define a deviation geodesic vector $\varsigma^a \equiv \lambda\,\delta\beta^a$ w.r.t. a null tetrad adapted to the path of the photons $(\ell^a, m^a, \bar{m}^a, n^a)$:

$$\varsigma^a = \varsigma\bar{m}^a + \bar{\varsigma}m^a + \eta\ell^a$$

$$\boxed{\ell\left(\ell\left(\boldsymbol{\mathcal{X}}\right)\right) = -Q\boldsymbol{\mathcal{X}}}$$

$$\boldsymbol{\mathcal{X}} = \begin{pmatrix} \varsigma \\ \bar{\varsigma} \end{pmatrix} \qquad Q = \begin{pmatrix} \Phi_{00} & \Psi_0 \\ \bar{\Psi}_0 & \Phi_{00} \end{pmatrix}$$

$$\Phi_{00} = -\frac{1}{2}R_{ab}\ell^a\ell^b \qquad \Psi_0 = C_{abcd}\ell^a m^b \ell^c m^d,$$

$$\mu = \frac{1}{(1-\kappa)^2 - \left(\gamma_1^2 + \gamma_2^2\right) + \omega^2} = \frac{\lambda_s}{\varsigma_{I2}\varsigma_{R1} - \varsigma_{I1}\varsigma_{R2}}$$

Gravitational lensing in Kerr spacetime I

Black hole lenses

$$\mathrm{d}s^2 = (1-\Phi)\,\mathrm{d}t^2 + 2\Phi a \sin^2(\theta)\,\mathrm{d}t\mathrm{d}\phi - \Sigma\Delta^{-1}\,\mathrm{d}r^2$$
$$- \Sigma\,\mathrm{d}\theta^2 - \left(r^2 + a^2 + \Phi a^2 \sin^2(\theta)\right)\sin^2(\theta)\,\mathrm{d}\phi^2$$

$$\Sigma = r^2 + a^2\cos(\theta)^2, \qquad \Delta = r^2 - 2rM + a^2, \qquad \Phi = 2Mr\Sigma^{-1}$$

- Lenses with angular momentum require a more subtle treatment than static and spherically symmetric ones since the deviation angle can not be obtained from a potential function [BDLS06, AKP11a, AKP11b, RCH17].

  We instead do not try to obtain a lens equation.

- In Kerr geometry we perform the combined integration of the *geodesic* and *geodesic deviation equations*:

$$\ell^a \nabla_a \ell^b = 0$$
$$\frac{d^2}{d\lambda^2}\begin{pmatrix}\varsigma \\ \bar{\varsigma}\end{pmatrix} = -\begin{pmatrix}\Phi_{00} & \Psi_0 \\ \bar{\Psi}_0 & \Phi_{00}\end{pmatrix}\begin{pmatrix}\varsigma \\ \bar{\varsigma}\end{pmatrix}$$

For black-holes $\Phi_{00} = 0$ but $\Psi_0 \neq 0$.

Gravitational lensing in Kerr spacetime II

Null Geodesics

- There are enough first integrals $\longrightarrow E, L_z, K, g_{ab}\ell^a\ell^b = 0$.

$$\ell_a = E\mathrm{dt}_a - \frac{\pm\sqrt{R(r)}}{\Delta}\mathrm{dr}_a - \left(\pm\sqrt{\Theta(\theta)}\right)\mathrm{d}\theta_a - L_z\mathrm{d}\phi_a \tag{1}$$

  Given a frame $(\mathrm{T}^a, \mathrm{X}^a, \mathrm{Y}^a, \mathrm{Z}^a)$ these constants are related to the position and to the angular coordinates (α_x, δ_z) on the sky of the observer.

- The construction of the most natural choice of frame in which Y^a points to the 'center' is not a trivial task to accomplish.

  We propose one based on the *center of mass null congruence* [AnM21].

Gravitational lensing in Kerr spacetime III

Ψ_0 and the null geodesic deviation equation

- Kerr is algebraically special of type-D, meaning that exists a *double principal null tetrad* $\left(\tilde{\ell}^a, \tilde{m}^a, \tilde{\bar{m}}^a, \tilde{n}^a\right)$ where the curvature is just

$$\widetilde{\Psi}_2 = -\frac{M}{\left(r - ia\cos(\theta)\right)^3},$$

all the other components of the Weyl tensor being zero:
$\widetilde{\Psi}_0 = \widetilde{\Psi}_1 = \widetilde{\Psi}_3 = \widetilde{\Psi}_4 = 0.$

Therefore, Ψ_0 must be proportional to $\widetilde{\Psi}_2$.

Gravitational lensing in Kerr spacetime IV

Relating $\widetilde{\Psi}_2$ with Ψ_0

- One is interested in Ψ_0 along each null geodesic bundle.
  The main difficulty being to build the tetrad adapted to the photon paths $(\ell^a, m^a, \bar{m}^a, n^a)$ reaching the observer: ℓ^a is known but m^a seems too hard to find.
- Looking at Lorentz transformations

$$(\tilde{\ell}^a, \tilde{m}^a, \bar{\tilde{m}}^a, \tilde{n}^a) \longrightarrow SO(3,1)^+ \longrightarrow (\ell^a, m^a, \bar{m}^a, n^a);$$

  one gets a relation between the tetrad completely described by two real (s, Z) and two complex (Λ, Γ).

$$\ell^a = Z\left(\tilde{\ell}^a + \Lambda\bar{\tilde{m}}^a + \bar{\Lambda}\tilde{m}^a + \Lambda\bar{\Lambda}\tilde{n}^a\right), \tag{2}$$

$$m^a = Z\Gamma\left(\tilde{\ell}^a + \Lambda\bar{\tilde{m}}^a + \bar{\Lambda}\tilde{m}^a + \Lambda\bar{\Lambda}\tilde{n}^a\right) + e^{is}\left(\tilde{m}^a + \Lambda\tilde{n}^a\right), \tag{3}$$

- Curvature transformation reveals that exact knowledge of Ψ_0 just requires to compute the product $Z\Lambda e^{is}$:

$$\boxed{\Psi_0 = 6\left(Z\Lambda e^{is}\right)^2 \widetilde{\Psi}_2.}$$

Conserved quantities for null geodesics in type-D spacetimes

Theorem ([WP70, Cha83])

If ℓ^a is an affinely parametrized null geodesic vector and m^a an orthogonal vector to ℓ^a which is parallelly propagated along it; then, in a type-D spacetime the following quantity is conserved along the geodesic:

$$\mathbb{K} = 2\left[(\ell^a\tilde{\ell}_a)(m^a\tilde{n}_a) - (\ell^a\tilde{m}_a)(m^a\bar{\tilde{m}}_a)\right]\widetilde{\Psi}_2^{-1/3}.$$

Corolary

If a restricted Lorentz transformation link tetrad $(\tilde{\ell}^a, \tilde{m}^a, \bar{\tilde{m}}^a, \tilde{n}^a)$ with $(\ell^a, m^a, \bar{m}^a, n^a)$; the conserved quantity along null geodesics $\mathbb{K}$ of the theorem is

$$\mathbb{K} = -2\left(Z\Lambda e^{is}\right)\widetilde{\Psi}_2^{-1/3}.$$

Gravitational lensing in Kerr spacetime VI

New and very simple expression for Ψ_0

New expression for Ψ_0

$$\Psi_0(r,\theta) = \frac{3M}{(r - ia\cos(\theta))^5}\left[\delta_z r_o - i\left(Ea\sin(\theta_o) + \alpha_x r_o\right)\right]^2 .$$

- Remarkably simple in terms of (α_x, δ_z), (r, θ) and θ_o.
- Exact and valid for any geodesic bundle.
- It allows very efficient computation of the combined system of geodesics + geodesic deviation equations.
- Straightforward derivation.

Gravitational lensing in Kerr spacetime VII

Previous expressions based on direct calculations

Previous for $\Re(\Psi_0)$

$$
\begin{aligned}
\Re(\Psi_{0*}) = \frac{1}{2(w-1)\left(p^{\hat{r}} - p^{\hat{\imath}}\right)^2} \Big\{ & Q_1 \Big(-3w\left(p_{\hat{\theta}}^2 - p_{\hat{\phi}}^2\right)^2 \\
& - 3p_{\hat{r}}^4 w + 2p_{\hat{r}}^3 \Big[3p^{\hat{\imath}} w + p_{\hat{\phi}} S(w-1) \Big] \\
& + 6p_{\hat{r}}^2 \Big[p_{\hat{\theta}}^2 - \left(p^{\hat{\imath}}\right)^2 w - p^{\hat{\imath}} p_{\hat{\phi}} S(w-1) - p_{\hat{\phi}}^2 (w+1) \Big] \\
& + 2p^{\hat{r}} \Big[p_{\hat{\phi}} S(w-1)\left(p_{\hat{\phi}}^2 - 3p_{\hat{\theta}}^2\right) \\
& + 3\left(p^{\hat{\imath}}\right)^3 w + 3\left(p^{\hat{\imath}}\right)^2 p_{\hat{\phi}} S(w-1) - 3p^{\hat{\imath}}(w+2)\left(p_{\hat{\theta}}^2 - p_{\hat{\phi}}^2\right) \Big] \\
& - 3\left(p^{\hat{\imath}}\right)^4 w - 2\left(p^{\hat{\imath}}\right)^3 p_{\hat{\phi}} S(w-1) \\
& + 6\left(p^{\hat{\imath}}\right)^2 \Big[p_{\hat{\theta}}^2 (w+1) - p_{\hat{\phi}}^2 \Big] - 2p^{\hat{\imath}} p_{\hat{\phi}} S(w-1)\left(p_{\hat{\phi}}^2 - 3p_{\hat{\theta}}^2\right) \Big) \\
& + 2\, Q_2\, p_{\hat{\theta}} \Big(3p_{\hat{\phi}} w \left(p_{\hat{\phi}}^2 - p_{\hat{\theta}}^2\right) \\
& + p_{\hat{r}}^3 S(1-w) + 3p_{\hat{r}}^2 \Big[p^{\hat{\imath}} S(w-1) + p_{\hat{\phi}}(w+2) \Big] \\
& - p_{\hat{r}} \Big[-S(w-1)\left(p_{\hat{\theta}}^2 - 3p_{\hat{\phi}}^2\right) + 3\left(p^{\hat{\imath}}\right)^2 S(w-1) \\
& + 6p^{\hat{\imath}} p_{\hat{\phi}}(w+2) \Big] + \left(p^{\hat{\imath}}\right)^3 S(w-1) + 3\left(p^{\hat{\imath}}\right)^2 p_{\hat{\phi}}(w+2) \\
& - p^{\hat{\imath}} S(w-1)\left(p_{\hat{\theta}}^2 - 3p_{\hat{\phi}}^2\right) \Big) \Big\},
\end{aligned}
$$

Previous for $\Im(\Psi_0)$

$$
\begin{aligned}
\Im(\Psi_{0*}) = \frac{1}{(w-1)\left(p^{\hat{r}} - p^{\hat{\imath}}\right)^2} \Big\{ & -Q_2 \Big(6p_{\hat{\theta}}^2 p_{\hat{\phi}}^2 w + p_{\hat{r}}^3 \Big[3p^{\hat{\imath}} w + p_{\hat{\phi}} S(w-1) \Big] \\
& + 3p_{\hat{r}}^2 \Big[p_{\hat{\theta}}^2 (w+1) - 2\left(p^{\hat{\imath}}\right)^2 w - p^{\hat{\imath}} p_{\hat{\phi}} S(w-1) - p_{\hat{\phi}}^2 \Big] \\
& + p_{\hat{r}} \Big[p_{\hat{\phi}} S(w-1)\left(p_{\hat{\phi}}^2 - 3p_{\hat{\theta}}^2\right) \\
& + 3\left(p^{\hat{\imath}}\right)^3 w + 3\left(p^{\hat{\imath}}\right)^2 p_{\hat{\phi}} S(w-1) - 3p^{\hat{\imath}}(w+2)\left(p_{\hat{\theta}}^2 - p_{\hat{\phi}}^2\right) \Big] \\
& - \left(p^{\hat{\imath}}\right)^3 p_{\hat{\phi}} S(w-1) \\
& + 3\left(p^{\hat{\imath}}\right)^2 \Big[p_{\hat{\theta}}^2 - p_{\hat{\phi}}^2 (w+1) \Big] - p^{\hat{\imath}} p_{\hat{\phi}} S(w-1)\left(p_{\hat{\phi}}^2 - 3p_{\hat{\theta}}^2\right) \Big) \\
& + Q_1\, p_{\hat{\theta}} \Big(3p_{\hat{\phi}} w \left(p_{\hat{\phi}}^2 - p_{\hat{\theta}}^2\right) \\
& + p_{\hat{r}}^3 S(1-w) + 3p_{\hat{r}}^2 \Big[p^{\hat{\imath}} S(w-1) + p_{\hat{\phi}}(w+2) \Big] \\
& - p_{\hat{r}} \Big[-S(w-1)\left(p_{\hat{\theta}}^2 - 3p_{\hat{\phi}}^2\right) + 3\left(p^{\hat{\imath}}\right)^2 S(w-1) \\
& + 6p^{\hat{\imath}} p_{\hat{\phi}}(w+2) \Big] + \left(p^{\hat{\imath}}\right)^3 S(w-1) + 3\left(p^{\hat{\imath}}\right)^2 p_{\hat{\phi}}(w+2) \\
& - p^{\hat{\imath}} S(w-1)\left(p_{\hat{\theta}}^2 - 3p_{\hat{\phi}}^2\right) \Big) \Big\}.
\end{aligned}
$$

Auxiliary functions

$$
Q_1 = \frac{r\left(r^2 - 3a^2\cos^2\theta\right)}{\rho^6}, \qquad Q_2 = \frac{a\cos\theta\left(3r^2 - a^2\cos^2\theta\right)}{\rho^6}, \qquad w = \frac{\Delta a^2 \sin^2\theta}{\left(r^2 + a^2\right)^2}, \qquad S = \frac{3a\sqrt{\Delta}\left(r^2 + a^2\right)\sin\theta}{\Sigma^2}.
$$

Synthetic images of accretion discs around black-holes

The EHT images of M87*

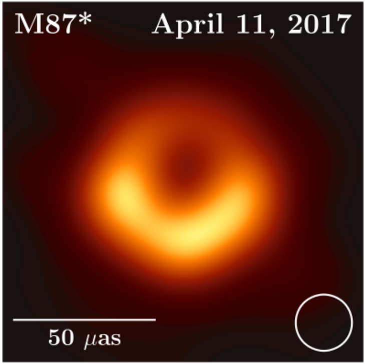

Figure: EHT image of M87* from observations on 2017 April 11 as a representative example of the images collected in the 2017 campaign. Credits: Image from Akiyama K. et al., 2019a, ApJ, 875, L1.

- Bright asymmetric ring at South location extending from East to West between PA $\in (80^o, 270^o)$ with a mean position angle at PA $\simeq 170^o$ [A$^+$19a, A$^+$19b].
- It has an approximate diameter $d \simeq 41\mu$as and a width $w \lesssim 20\mu$as [A$^+$19b].
- The asymmetric ring seems to have two distinguished bright regions over imposed on it.
- An observed brightness temperature in radio wavelengths in the range of $10^9 - 10^{10}K$ as expected [Ho99]; with a central depression, the main signature for the BH hypothesis.

M87* image II

- EHT observations bring us closer to the possibility of testing models on very compact sources and the surrounding material in horizon scales: composition of the matter, geometry, emission profile, etc.
- Current resolutions and intrinsic limitations allow for some degeneracy in the images [A+19a].

Other observations from M87*

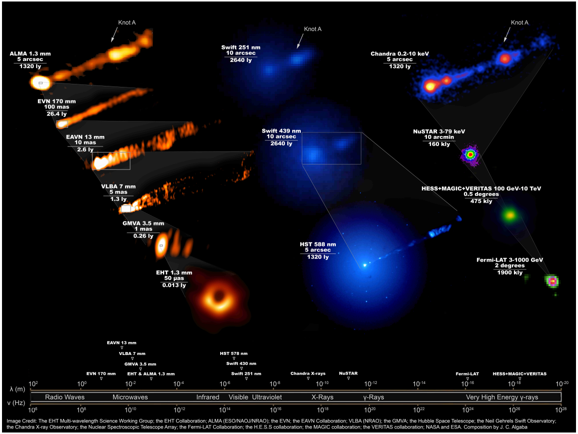

Figure: Composite image showing how the M87 system looked, across the entire electromagnetic spectrum, during the Event Horizon Telescope's April 2017 campaign. Credits: Image taken from the EHT blog page `https://eventhorizontelescope.org/blog/telescopes-unite-unprecedented-observations-famous-black-hole` (see the full list of credits also there).

About the M87* system

- M87 belongs to the class of LLAGN's usually associated to hot accretion flows, in which the accreting material is usually described as a plasma having two temperatures regions associated to ions and electrons.
- The emission is thought to be synchroton radiation coming from a *geometrically thick* but *optically thin* accretion disk. So, its emission is not a blackbody.
- To give account of the large scale jet the hypothesis of a SMBH is the most promising one [BZ77].

In fact, the EHT observations reveal that emission at 1.3mm ($\sim$230GHz) is weakly absorbed.

The M87* system III

Simulating images of M87*

- Physical models combine a hot and highly ionized plasma over a curved background; the treatment then recurs to the use of general relativistic magnetohydrodynamical (GRMHD) simulations together with ray tracing algorithms in order to produce images.
- The EHT Collaboration employed two kind of simulations essentially distinguished by the magnetic flux at the horizon: the so called “SANE” $\phi \sim 1$ and the “MAD” strongly magnetized $\phi \sim 15$ [A$^+$19a].

The M87* system IV

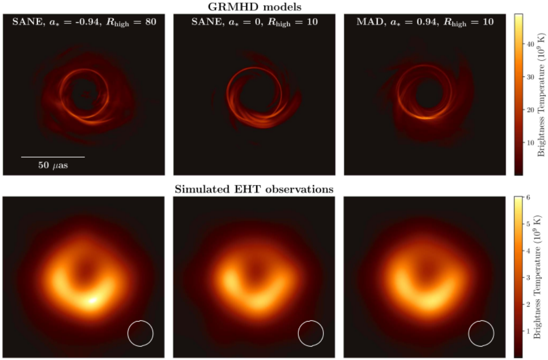

Figure: Three examples of very different models from the image library employed by the EHT Collaboration for the April 11 images. Credits: Image taken from [A+19a].

- The crescent bright region is ascribed to the presence of a bright ring which is a persistent feature in the simulations.

This ring has been associated with the so-called photon ring of the BH.

Numerical implementation I

Numerical code

- The code works by running the integration from the observer position until one of the following conditions take place; the null geodesic:
  1. crosses the event horizon
  2. hits the equatorial plane in the regions where the accretion disk is defined or,
  3. hits the equatorial plane in the outer regions.

Let us note that the above procedure implies that we are considering that the null geodesics are emanating from the equatorial accretion disk; which does not exclude the possible presence of a thick and more tenuous disk which is optically thin surrounding the BH

Simple model of emission for M87* I

Basic model

- $M = 6.6 \times 10^9 M_\odot$ $\quad a = 0.98M$ $\quad d_l = 16.7\text{Mpc}$
- The tilt and the PA of the spin axis is indicated by the jet; so we only have the freedom to consider aligned or anti-aligned cases.

- Model inspired from [MFS16]
- Inner hot disk: $r_{\text{hor}} < r < r_{\text{in}}$ ($r_{\text{in}} \sim 16\mu$as and $\Theta_e = 7$)
- Outer warm disk: $r_{\text{in}} < r < r_{\text{out}}$ ($r_{\text{out}} \sim 45\mu$as and $\Theta_e = 0.2$)
- Ambient temperature: $\Theta_e = 0.05$
- We consider the plasma in prograde geodesic motion.

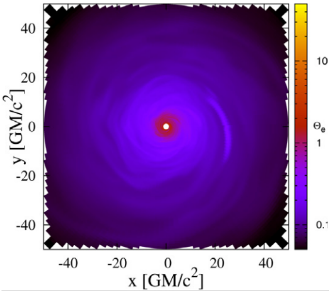

Figure: Two temperature model for the midplane disk. Credits: Image from [MFS16].

Results I

Anti-aligned with respect to the jet

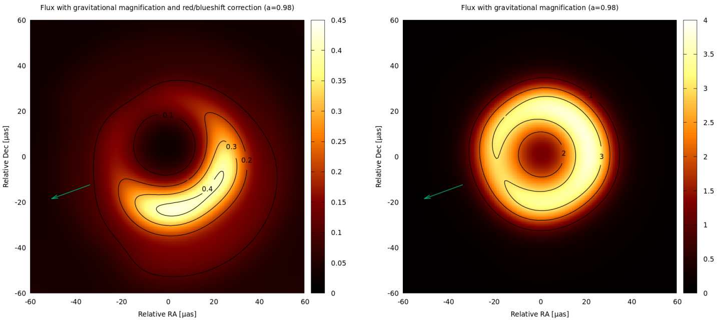

- The effect is dominated by the red/blueshift contribution.
- The bright ring has a shorter extension with respect to the EHT (PA $\in (135^o, 290^o)$) and the mean PA changes about 50^o.
- It has similar values for the diameter d and the width w than those measured by the Collaboration.

Aligned with respect to the jet

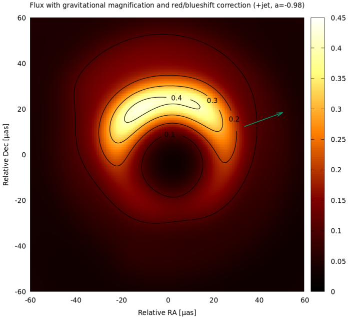

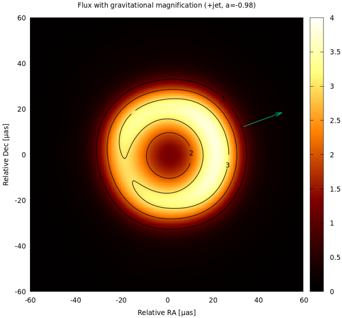

- The bright crescent indicates the spin direction and PA and not the sense of motion of the accretion disk.

Results III

Changes with the spin parameter

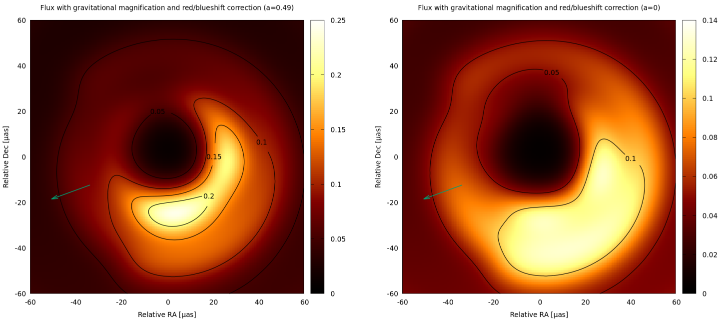

- Lower spin are disfavored.

Results IV

Two temperature disk model with an asymmetric bar

- To give account of the two bright spots within the ring, we included in our model an emission component intended to balance the lack of brightness at the south-west location.
- The most simple modification to achieve that goal is a bar like structure at appropriate angular direction and at a higher temperature than the disk.
- We do not intend to ascribe a clear physical origin to a bar like emission model; instead we just investigate which are the appropriate simple geometries that can be successful to describe the emitter.

Results V

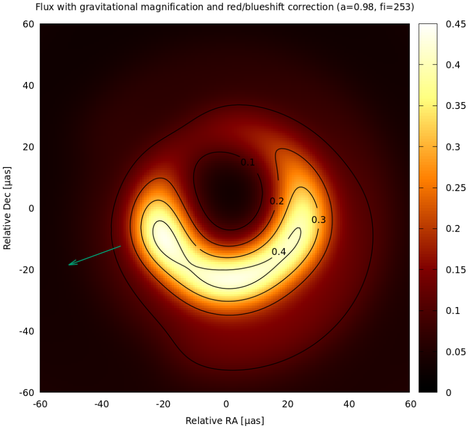

Flux with gravitational magnification and red/blueshift correction (a=0.98, fi=253)
Relative Dec [µas]
Relative RA [µas]
60
40
20
0
-20
-40
-60
-60
-40
-20
0
20
40
60
0.1
0.2
0.3
0.4
0.45
0.4
0.35
0.3
0.25
0.2
0.15
0.1
0.05
0

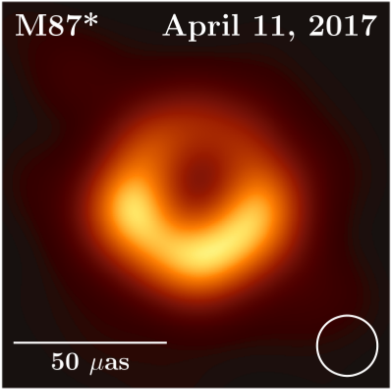

M87*
April 11, 2017
50 μas

Comparison of images II

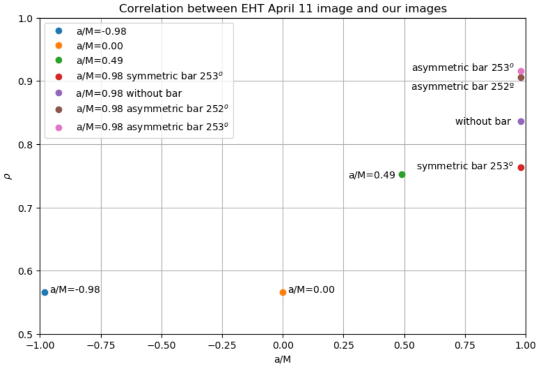

Figure: Correlation coefficient between the EHT April 11 image with our images as a function of the angular parameter a/M.

Summary and final comments

- EHT observations are bringing us closer to the possibility of testing models on very compact sources and the surrounding material in their immediate neighborhood.
- Their template bank of simulations shows the persistent presence of a bright ring that would explain the salient features of the blurred images. This ring has been associated with the so-called photon ring.
- We have approached the simulation process of images recurring to the full set of geodesic and geodesic deviation equation, and making use of a very simple geometric model for the emission from the accretion disk. With the present level of resolution our simple modeling can be employed to give a very good reconstruction of the image generated from the observed EHT data.
- This approach do not emphasizes the effects of the photon ring. Instead, the proper signatures imprinted on the final image should be almost completely associated to the emission model and red/blueshift contributions. Our simulation do not consider enhanced intensity due to the contribution of photons paths with many turns around the SMBH as in fully optically thin disks.

Thanks for your attention!

References I

Kazunori Akiyama et al.
First M87 Event Horizon Telescope Results. I. The Shadow of the Supermassive Black Hole.
Astrophys. J., 875(1):L1, 2019.

Kazunori Akiyama et al.
First M87 Event Horizon Telescope Results. IV. Imaging the Central Supermassive Black Hole.
Astrophys. J., 875(1):L4, 2019.

Amir B. Aazami, Charles R. Keeton, and A. O. Petters.
Lensing by Kerr Black Holes. I: General Lens Equation and Magnification Formula.
J. Math. Phys., 52:092502, 2011.

Amir B. Aazami, Charles R. Keeton, and A. O. Petters.
Lensing by Kerr Black Holes. II: Analytical Study of Quasi-Equatorial Lensing Observables.
J. Math. Phys., 52:102501, 2011.

References II

Marcos A. Argañaraz and Osvaldo M. Moreschi.
Double null coordinates for Kerr spacetime.
Phys. Rev. D, 104(2):024049, 2021.

V. Bozza, F. De Luca, and G. Scarpetta.
Kerr black hole lensing for generic observers in the strong deflection limit.
Phys. Rev., D74:063001, 2006.

Ezequiel F. Boero and Osvaldo M. Moreschi.
Gravitational lens optical scalars in terms of energy–momentum distributions in the cosmological framework.
MNRAS, 475(4):4683–4703, January 2018.

Ezequiel F. Boero and Osvaldo M. Moreschi.
Efficient gravitational lens optical scalars calculation of black holes with angular momentum.
MNRAS, 492(3):3763–3778, March 2020.

References III

Ezequiel F. Boero and Osvaldo M. Moreschi.
Strong gravitational lens image of the M87 black hole with a simple accreting matter model.
MNRAS, 507(4):5974–5990, November 2021.

R. D. Blandford and R. L. Znajek.
Electromagnetic extraction of energy from Kerr black holes.
MNRAS, 179:433–456, May 1977.

Gabriel Crisnejo, Emanuel Gallo, Ezequiel Boero, and Osvaldo M. Moreschi.
Perturbative and numerical approach to plasma strong lensing.
Accepted for publication in Phys. Rev. D, 12 2022.

Subrahmanyan Chandrasekhar.
The mathematical theory of black holes.
Oxford University Press, 646 p., Oxford, 1983.

References IV

Emanuel Gallo and Osvaldo Moreschi.
Peculiar anisotropic stationary spherically symmetric solution of Einstein equations.
Mod.Phys.Lett., A27:1250044, 2012.

Luis C. Ho.
The spectral energy distributions of low-luminosity active galactic nuclei.
Astrophys. J., 516:672–682, 1999.

Monika Moscibrodzka, Heino Falcke, and Hotaka Shiokawa.
General relativistic magnetohydrodynamical simulations of the jet in M 87.
Astron. Astrophys., 586:A38, 2016.

Arianna I. Renzini, Carlo R. Contaldi, and Alan Heavens.
Mapping weak lensing distortions in the Kerr metric.
Phys. Rev., D95(12):124047, 2017.

M. Walker and R. Penrose.
On quadratic first integrals of the geodesic equations for type [22] spacetimes.
Commun. Math. Phys., 18:265–274, 1970.